Cell. Mol. Life Sci. (2013) 70:4181–4195
DOI 10.1007/s00018-013-1385-2

Cellular and Molecular Life Sciences

RESEARCH ARTICLE

Extracellular wildtype and mutant SOD1 induces ER–Golgi pathology characteristic of amyotrophic lateral sclerosis in neuronal cells

Vinod Sundaramoorthy · Adam K. Walker · Justin Yerbury · Kai Ying Soo · Manal A. Farg · Vy Hoang · Rafaa Zeineddine · Damian Spencer · Julie D. Atkin

Received: 25 February 2013 / Revised: 3 May 2013 / Accepted: 23 May 2013 / Published online: 14 June 2013

Abstract Amyotrophic lateral sclerosis (ALS) is a fatal and rapidly progressing neurodegenerative disorder and the majority of ALS is sporadic, where misfolding and aggregation of Cu/Zn-superoxide dismutase (SOD1) is a feature shared with familial mutant-SOD1 cases. ALS is characterized by progressive neurospatial spread of pathology among motor neurons, and recently the transfer of extracellular, aggregated mutant SOD1 between cells was demonstrated in culture. However, there is currently no evidence that uptake of SOD1 into cells initiates neurodegenerative pathways reminiscent of ALS pathology. Similarly, whilst dysfunction to the ER–Golgi compartments is increasingly implicated in the pathogenesis of both sporadic and familial ALS, it remains unclear whether misfolded, wildtype SOD1 triggers ER–Golgi dysfunction. In this study we show that both extracellular, native wildtype and mutant SOD1 are taken up by macropinocytosis into neuronal cells. Hence uptake does not depend on SOD1 mutation or misfolding. We also demonstrate that purified mutant SOD1 added exogenously to neuronal cells inhibits protein transport between the ER–Golgi apparatus, leading to Golgi fragmentation, induction of ER stress and apoptotic cell death. Furthermore, we show that extracellular, aggregated, wildtype SOD1 also induces ER–Golgi pathology similar to mutant SOD1, leading to apoptotic cell death. Hence extracellular misfolded wildtype or mutant SOD1 induce dysfunction to ER–Golgi compartments characteristic of ALS in neuronal cells, implicating extracellular SOD1 in the spread of pathology among motor neurons in both sporadic and familial ALS.

Keywords Extracellular · SOD1 · ALS · Endoplasmic reticulum · Golgi

Electronic supplementary material The online version of this article (doi:10.1007/s00018-013-1385-2) contains supplementary material, which is available to authorized users.

V. Sundaramoorthy · A. K. Walker · K. Y. Soo · M. A. Farg · V. Hoang · D. Spencer · J. D. Atkin (✉)
Department of Biochemistry, Latrobe Institute for Molecular Science, La Trobe University, Bundoora, Melbourne, VIC 3086, Australia
e-mail: j.atkin@latrobe.edu.au

A. K. Walker
Center for Neurodegenerative Disease Research, School of Medicine, University of Pennsylvania, Philadelphia, PA 19104, USA

J. Yerbury · R. Zeineddine
School of Biological Sciences, University of Wollongong, Wollongong, NSW 2522, Australia

J. D. Atkin
Department of Florey Neuroscience, University of Melbourne, Parkville, VIC 3010, Australia

Introduction

Amyotrophic lateral sclerosis (ALS) is a neurodegenerative disorder with focal onset followed by progressive spread throughout surrounding upper and lower motor neurons. The intercellular transfer of misfolded proteins has recently been demonstrated in several neurodegenerative diseases, including ALS [1–3], and it has been suggested that this mechanism is responsible for the progressive spread of pathology. Mutations in SOD1 (Cu/Zn-superoxide dismutase) cause 20 % of familial ALS, and these cases display similar clinical features and pathogenesis to sporadic ALS, which accounts for 90 % of all ALS cases. Misfolded and aggregated SOD1 is present in both familial and sporadic ALS, but its pathobiology remains unclear [4, 5].

However, endoplasmic reticulum (ER) stress and fragmentation of the Golgi apparatus are well-described features in human ALS patients as well as in animal and cellular disease models [6–9]. ER stress is triggered initially in the most vulnerable motor neurons during early disease stages in several lines of transgenic mutant SOD1 mice, thus implying an active role in neurodegeneration [8].

Wildtype SOD1 ($SOD1^{WT}$) misfolds upon pathogenic triggers such as oxidative stress, and misfolded $SOD1^{WT}$ exhibits similar toxic properties to mutant SOD1 [4]. Oxidized, misfolded $SOD1^{WT}$ is present in the intracellular inclusions in motor neurons of sporadic ALS patients [5, 10]. Furthermore, recently it was shown that transgenic overexpression of $SOD1^{WT}$ causes ALS in mice [11]. Together these data suggest that misfolded $SOD1^{WT}$ could play a similar role to mutant SOD1 in the pathogenesis of sporadic ALS. There is accumulating evidence that secreted, extracellular SOD1, which is misfolded either due to mutation or cellular stress, could be a toxic factor spreading neurodegeneration among motor neurons in ALS. SOD1 is secreted by neuronal cells [12, 13] and is present in the cerebrospinal fluid (CSF) of ALS patients [14, 15]. Aggregated mutant SOD1 can be taken up by cells via macropinocytosis which triggers subsequent aggregation of natively folded SOD1 [1]. Similarly, extracellular misfolded $SOD1^{WT}$ induces cell death [16] and overexpression of $SOD1^{WT}$ induces misfolding of natively folded SOD1 in human but not mouse neuronal cell lines, demonstrating species specificity in the transfer of misfolding [17]. Furthermore, therapeutic strategies targeting extracellular SOD1 using antibodies specific to misfolded SOD1, delay disease progression in mutant SOD1 transgenic mice [18–20]. However, there is currently no evidence to show that uptake of extracellular misfolded SOD1 into neuronal cells initiates neurodegenerative pathways reminiscent of ALS pathology. It also remains unclear if both natively folded and misfolded forms of $SOD1^{WT}$ and mutant SOD1 can be taken up by neurons.

ER stress triggers the unfolded protein response (UPR), a set of signaling pathways that activate sensor proteins including inositol requiring kinase 1 (IRE1), activating transcription factor 6 (ATF-6) and x-box binding protein 1 (Xbp1) [21]. Activation of UPR leads to down-regulation of general protein expression and upregulation of specific ER chaperones including immunoglobulin binding protein (BiP) and protein disulfide isomerase (PD1). BiP plays a key role in regulating induction of ER stress [22]. This leads to the upregulation and activation of IRE1, which mediates the splicing of Xbp1. Whilst initially protective, prolonged ER stress initiates apoptosis by activating CHOP (C/EBP homologous protein) [21], a transcription factor which translocates to the nucleus upon activation. Whilst ER stress is now recognized as an important pathogenic feature of ALS, the mechanism by which mutant SOD1 activates the UPR is not fully defined, but includes binding of mutant SOD1 to Derlin-1 at least by symptom onset in transgenic SOD1 mice [22]. Conventionally ER stress is triggered when misfolded proteins accumulate within ER, but SOD1 is predominately cytoplasmic [23]. However, ER stress can also be triggered by inhibition of protein transport between ER and Golgi apparatus [24, 25]. Inhibition of ER–Golgi transport implies disruption to the secretory pathway, and Golgi fragmentation is another pathological feature of ALS, observed in both human patients and cellular and animal disease models [9, 26]. Likewise, the Golgi apparatus can fragment due to defects in ER to Golgi trafficking [27].

In this study, we examined whether extracellular, misfolded $SOD1^{WT}$ and mutant G93A SOD1 ($SOD1^{G93A}$) activate cellular events characteristic of ALS pathology after uptake into neurons. Aggregated $SOD1^{WT}$ and $SOD1^{G93A}$ proteins were taken up into mouse NSC-34 and human SH-SY5Y neuronal cells, leading to ER stress, Golgi fragmentation, and inhibition of ER–Golgi protein trafficking. Apoptotic cell death was also triggered in SH-SY5Y cells. Furthermore, natively folded $SOD1^{WT}$ was taken up by both cell lines, demonstrating that uptake is not specific to mutation or misfolding of SOD1. Hence extracellular misfolded $SOD1^{WT}$ and $SOD1^{G93A}$ induce cellular pathology characteristic of ALS, providing evidence for cell-to-cell transfer of SOD1 mediated neurotoxicity.

Results

Uptake of extracellular $SOD1^{WT}$ and $SOD1^{G93A}$ by neuronal cells

In order to examine the cell-to-cell propagation of SOD1, we first analyzed the uptake of extracellular SOD1 by mouse (NSC-34) motor neuron-like cell lines. Wildtype human SOD1 ($SOD1^{WT}$) and ALS-linked human mutant $SOD1^{G93A}$ proteins were expressed in bacteria and purified to homogeneity as previously described [28]. Both proteins were metallated to the extent that they were enzymically active [28]. Each protein was labeled with Alexa Fluor 488 dye and then added to the culture medium of NSC-34 cells at a concentration of 2 μg/mL. Using fluorescence microscopy, the uptake of both labeled $SOD1^{WT}$ and $SOD1^{G93A}$ was observed after 48 h (Fig. 1a), demonstrating that both $SOD1^{WT}$ and mutant SOD1 can be taken up by neuronal NSC-34 cells. The formation of prominent inclusion-like structures was detected specifically after uptake of extracellular mutant SOD1 but not $SOD1^{WT}$ in NSC-34 cells. Furthermore, inhibitors of

macropinocytosis [5-(*N*-ethyl-*N*-isopropyl)amiloride (EIPA) and rottlerin] blocked the uptake of both $SOD1^{WT}$ and $SOD1^{G93A}$ by NSC-34 cells, in contrast to inhibitors of clathrin mediated endocytosis [genistein and chlorpromazine hydrochloride (CPZ); Fig. S1]. This suggests that both $SOD1^{WT}$ and $SOD1^{G93A}$ are taken up by macropinocytosis into NSC-34 cells, as previously reported for aggregated mutant SOD1 [1].

We then examined the uptake of extracellular SOD1 prepared in a mammalian baculovirus expression system. We transiently expressed GST-tagged $SOD1^{WT}$ and $SOD1^{G93A}$ in Sf9 insect cells, which resulted in secretion of SOD1 into the medium due to the presence of the AKH signal peptide [29]. Expression and secretion of SOD1 was confirmed at 48 h post-transfection by immunoblotting of the conditioned Sf9 medium with an anti-GST antibody (Fig. S2A). Furthermore, zymography confirmed that both mutant and $SOD1^{WT}$ retained enzymatic activity in the conditioned media, demonstrating that both proteins were in their metallated, native form (Fig. S2B). The Sf9 conditioned media was then applied to untransfected NSC-34 cells for 48 h. Immunocytochemistry using an anti-GST antibody revealed that GST-tagged $SOD1^{WT}$ and $SOD1^{G93A}$ were taken up by NSC-34 cells (Fig. 1b). However, there was no uptake in NSC-34 cells treated with conditioned medium from insect cells expressing GST only, demonstrating that there was some specificity in the uptake for SOD1. In cells treated with $SOD1^{WT}$ conditioned medium, the fluorescence was uniform and dispersed throughout the cells. However, in cells treated with mutant $SOD1^{G93A}$, prominent fluorescent structures reminiscent of inclusions were present (Fig. 1b). Hence both natively folded $SOD1^{WT}$ and $SOD1^{G93A}$ present in insect cell conditioned media were taken up by NSC-34 cells, and the uptake of $SOD1^{G93A}$ resulted in the formation of intracellular SOD1 inclusions.

Uptake of extracellular recombinant mutant SOD1 activates ER stress in mouse NSC-34 cells

We next examined whether the uptake of extracellular mutant SOD1 activates ER stress in NSC-34 cells. We first examined whether the early phase of the UPR is activated in cells treated with extracellular SOD1. Immunoblotting for UPR markers IRE1, BiP and Xbp1 revealed an upregulation of all three proteins in cells treated with mutant $SOD1^{G93A}$ compared to untreated cells or those treated with $SOD1^{WT}$ (Fig. 1c, d; threefold, $P < 0.01$). Hence the early phases of UPR are induced in cells treated with extracellular mutant $SOD1^{G93A}$. We then examined cells for the later, pro-apoptotic phase of UPR using immunocytochemistry for nuclear CHOP [30, 31]. After 72 h treatment, a significant increase in nuclear CHOP immunoreactivity was observed in NSC-34 cells treated with $SOD1^{G93A}$ compared to untreated and $SOD1^{WT}$ treated cells (Fig. 1e, f; twofold, $P < 0.001$). Hence the pro-apoptotic phase of UPR was also triggered in mutant SOD1 treated cells. These findings were confirmed in NSC-34 cells treated with Sf9 cell conditioned media. A significant upregulation in nuclear CHOP immunoreactivity was detected on treatment with Sf9 medium from $SOD1^{G93A}$ expressing cells compared to $SOD1^{WT}$ and GST alone expressing cells (Fig. 1g; twofold, $P < 0.001$). Hence the uptake of extracellular mutant SOD1 expressed in either bacterial or a baculovirus system specifically induces ER stress, including pro-apoptotic CHOP, in NSC-34 cells.

Uptake of extracellular aggregated $SOD1^{WT}$ and $SOD1^{G93A}$ by SH-SY5Y human neuronal cells

We next asked whether uptake of aggregated/misfolded $SOD1^{WT}$ could induce ALS-like pathology in neuronal cells. For this purpose a human neuroblastoma cell line (SH-SY5Y) was used due to the previously reported species specificity in seeding $SOD1^{WT}$ aggregation [17]. Aggregated recombinant $SOD1^{WT}$ and mutant $SOD1^{G93A}$ proteins were prepared by treatment with 5 mM EDTA and 50 mM DTT to remove metal ions and reduce the native Cys57-Cys146 SOD1 disulfide bond, respectively, as described previously [28, 32–34]. The aggregated proteins ($aggSOD1^{WT}$, $aggSOD1^{G93A}$) and native $SOD1^{WT}$ and $SOD1^{G93A}$ were then labeled with Alexa Fluor 488 dye. Silver staining of non-denaturing native gel and denaturing SDS-PAGE gel revealed that both $SOD1^{WT}$ and $SOD1^{G93A}$ formed SDS-stable high molecular weight aggregates (Fig. 2a, b).

Labeled $aggSOD1^{WT}$ and $aggSOD1^{G93A}$, and unaggregated $SOD1^{WT}$ and $SOD1^{G93A}$ for comparison were then added to the culture medium of SH-SY5Y cells at a concentration of 2 μg/mL. Fluorescence microscopy revealed that 48 h after treatment, SH-SY5Y cells had taken up both aggregated and unaggregated $SOD1^{WT}$ and $SOD1^{G93A}$ from the culture medium (Fig. 2c). Differential interference contrast (DIC) microscopy revealed the formation of membrane ruffles in all cases, consistent with a macropinocytosis mechanism for uptake of SOD1, as previously reported for mutant SOD1 aggregates [1] (Fig. 2c). In cells treated with $SOD1^{G93A}$, $aggSOD1^{WT}$ and $aggSOD1^{G93A}$ intracellular fluorescent inclusions were formed (20–30 % of cells; Fig. 2d). Surprisingly, in a small proportion of cells (7 %) treated with unaggregated native $SOD1^{WT}$, inclusions were also present (Fig. 2d), which were never observed in murine NSC-34 cells (Fig. 1a, b). Intracellular higher molecular weight SOD1 aggregates were also present in cell lysates, which were harvested after 0.125 % trypsin treatment of the cells, to digest residual extracellular SOD1 aggregates

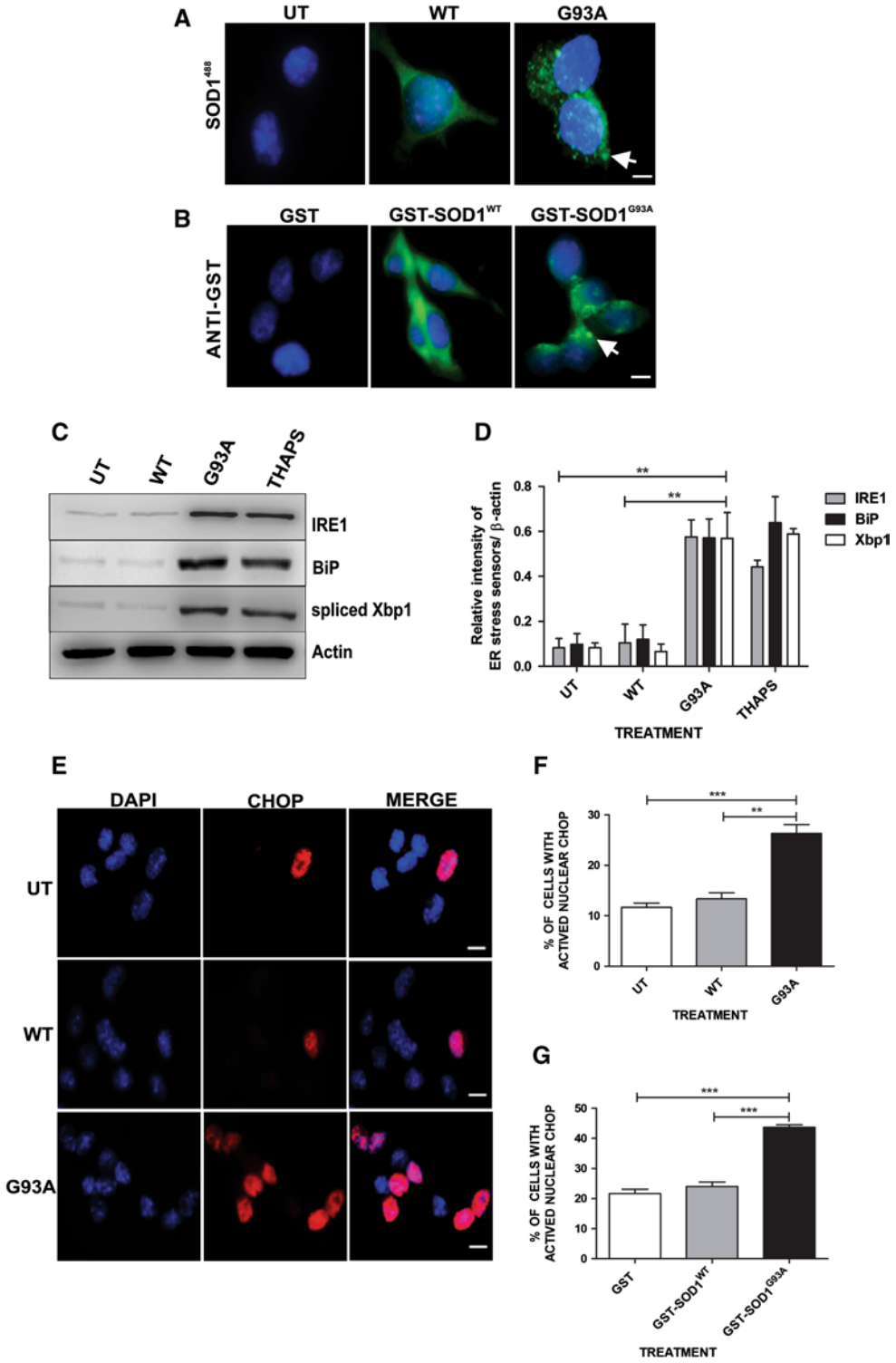

(Fig. 2e). Endogenous human SOD1 was clearly present in untreated cells (Fig. 2e). However, in all cells treated with extracellular SOD1, reduced levels of endogeneous SOD1 was observed, and a corresponding increase in the levels of high molecular weight aggregates was detected. This finding implies that recruitment of endogenous SOD1 into higher molecular weight aggregates has occurred in cells treated with aggregated $SOD1^{WT}$ and mutant SOD1. Also, consistent with the microscopy findings, in unaggregated $SOD1^{WT}$ treated cell lysates, SOD1 aggregates were observed, although these aggregates ran at a faster mobility than those formed by mutant SOD1, suggesting they

◀ **Fig. 1** Uptake of extracellular mutant $SOD1^{G93A}$ triggers ER stress in mouse NSC-34 cells. **a** Recombinant $SOD1^{WT}$ and $SOD1^{G93A}$ (2 μg/mL) labeled with Alexa Fluor 488 dye (*green*) are taken up by NSC-34 cells 48 h after addition to medium. Nuclei are stained with DAPI (*blue*). *White arrows* show the formation of inclusion-like structures in cells treated with extracellular $SOD1^{G93A}$. **b** Extracellular GST-tagged $SOD1^{WT}$ and $SOD1^{G93A}$ (GST-$SOD1^{WT}$, GST-$SOD1^{G93A}$) are taken up by NSC-34 cells. Insect cell (Sf9) conditioned medium containing GST-$SOD1^{WT}$, GST-$SOD1^{G93A}$ or GST only control (100 μg total protein) was added to NSC-34 cells for 48 h. Cells were then fixed and immunostained with anti-GST antibody (*green*). No immunoreactivity was observed in cells treated with GST alone (GST) in contrast to GST-SOD1 treated cells. *White arrow* shows the formation of inclusion-like structures in cells treated with extracellular GST-$SOD1^{G93A}$. **c** Immunoblotting reveals upregulation of UPR markers IRE1, BiP, and spliced Xbp1 in NSC-34 cells 72 h after treatment with recombinant purified $SOD1^{G93A}$, in contrast to cells treated with recombinant $SOD1^{WT}$ and untreated (UT) cells (20 μg/lane). As a positive control NSC-34 cells were treated with 10 μM thapsigargin to induce ER stress (THAPS) for 1 h before lysis. β-actin was used as a loading control. **d** Densitometric analysis of the immunoblots relative to β-actin intensity confirms upregulation of all three UPR markers in NSC-34 cells treated with recombinant $SOD1^{G93A}$. **e** Representative images showing increased nuclear immunoreactivity to pro-apoptotic, ER stress-specific CHOP (*red*) in NSC-34 cells treated with $SOD1^{G93A}$ for 72 h. Nuclei are stained with DAPI (*blue*). **f** Quantification of NSC-34 cells containing nuclear immunoreactivity to CHOP 72 h after treatment with recombinant, purified SOD1 ($SOD1^{WT}$, $SOD1^{G93A}$) and untreated cells (UT). **g** Quantification of NSC-34 cells containing nuclear immunoreactivity to CHOP 72 h after treatment with Sf9 insect cell conditioned medium containing GST-SOD1 (GST-$SOD1^{WT}$, GST-$SOD1^{G93A}$) or GST alone. Results are expressed as mean ± SEM; $n = 3$; $^{**}P < 0.01$, $^{***}P < 0.001$ versus $SOD1^{WT}$ and untreated cells (UT) (**f**) or $SOD1^{WT}$ or GST treated cells (**g**) as indicated by one-way ANOVA with Tukey's post-test, $n = 3$. All *scale bars* represent 10 μm

are smaller than those in other cell populations. Hence misfolded/aggregated $SOD1^{WT}$ and mutant SOD1 are taken up by human neuronal cells, leading to intracellular SOD1 aggregation and possible recruitment of endogenous SOD1. Induction of SOD1 aggregation by natively folded $SOD1^{WT}$ was also detected in a small proportion of cells.

Uptake of extracellular aggregated $SOD1^{WT}$ and $SOD1^{G93A}$ activates ER stress in SH-SY5Y cells

We next examined whether ER stress is activated in SH-SY5Y cells treated with extracellular $SOD1^{G93A}$, $aggSOD1^{WT}$ and $aggSOD1^{G93A}$ for 72 h. Immunoblotting for IRE1, BiP and spliced Xbp1, revealed that the UPR was induced (Fig. 3a, b; twofold, $P < 0.01$) in SH-SY5Y cells treated with aggregated and unaggregated $SOD1^{G93A}$ compared to untreated cells, consistent with the findings in NSC-34 cells. Furthermore, in cells treated with $aggSOD1^{WT}$, induction of the UPR was also observed, demonstrating that $SOD1^{WT}$ can also trigger ER stress when misfolded. Surprisingly we also observed a slight but significant upregulation of Xbp1 ($P < 0.05$) in cells treated with unaggregated $SOD1^{WT}$ compared to untreated cells. Similarly, using immunocytochemistry, a significant increase in nuclear CHOP in SH-SY5Y cells treated with $SOD1^{G93A}$, $aggSOD1^{WT}$ and $aggSOD1^{G93A}$ treated cells compared to untreated cells was detected (Fig. 3c, d; threefold, $P < 0.001$). Hence uptake of extracellular aggregated SOD1 induces the ER stress-specific pro-apoptotic phase of UPR in SH-SY5Y cells, similar to mutant SOD1. Consistent with the immunoblotting results, we observed a modest but significant increase in nuclear CHOP immunoreactivity in cells treated with unaggregated $SOD1^{WT}$ ($P < 0.05$) compared to untreated cells. In contrast, neither bacterial nor baculovirus $SOD1^{WT}$ induced ER stress in NSC-34 cells (Fig. 1c). Hence extracellular, native $SOD1^{WT}$ induces ER stress in the SH-SY5Y human cell line but not the NSC-34 mouse neuronal cell line.

Extracellular aggregated $SOD1^{WT}$ and $SOD1^{G93A}$ inhibits ER to Golgi protein trafficking and induces Golgi fragmentation

We next examined whether extracellular misfolded or mutant SOD1 could also inhibit ER to Golgi protein trafficking. Vesicular stomatitis virus glycoprotein ts045 (VSVG-ts045) is a widely employed marker used to examine ER–Golgi transport [35]. VSVG-ts045 misfolds and is retained in the ER at 40 °C, but is transported to the Golgi apparatus at the permissive temperature of 32 °C [35]. We first examined ER–Golgi transport in SH-SY5Y cells transfected with SOD1 proteins linked to EGFP [6, 12] and VSVG-ts045 mCherry, to confirm that intracellular mutant SOD1 can inhibit ER–Golgi trafficking in this cell line. VSVG-ts045 was detected immunocytochemically using markers of the ER (calnexin) and Golgi (GM130) and its co-localization with each marker was quantified using Mander's coefficient [36]. At 32 °C, VSVG-ts045 was transported to the Golgi in untransfected cells and in cells expressing $SOD1^{WT}$ (Fig. S3A). However, in cells expressing mutant SOD1 (Fig. S3A) most VSVG-ts045 remained in the ER and significantly less (~50 %) was transported to the Golgi (Fig. S3B; $P < 0.01$). Hence ER–Golgi trafficking is inhibited by intracellular mutant SOD1 in the SH-SY5Y cell line (Fig. S3A, S3B). We next examined ER–Golgi transport in cells treated with extracellular SOD1 proteins. SH-SY5Y cells were transiently transfected with VSVG-ts045 mCherry. At 24 h post-transfection, 2 μg/mL of purified, labeled $SOD1^{WT}$, $SOD1^{G93A}$, $aggSOD1^{WT}$ and $aggSOD1^{G93A}$ were added to the SH-SY5Y medium for another 48 h. Transport of VSVG-ts045 from the ER to Golgi was then examined using immunocytochemistry to calnexin and GM130 as above. Quantification of the degree of co-localization of VSVG-ts045 with ER and Golgi compartments using Mander's coefficient was then performed.

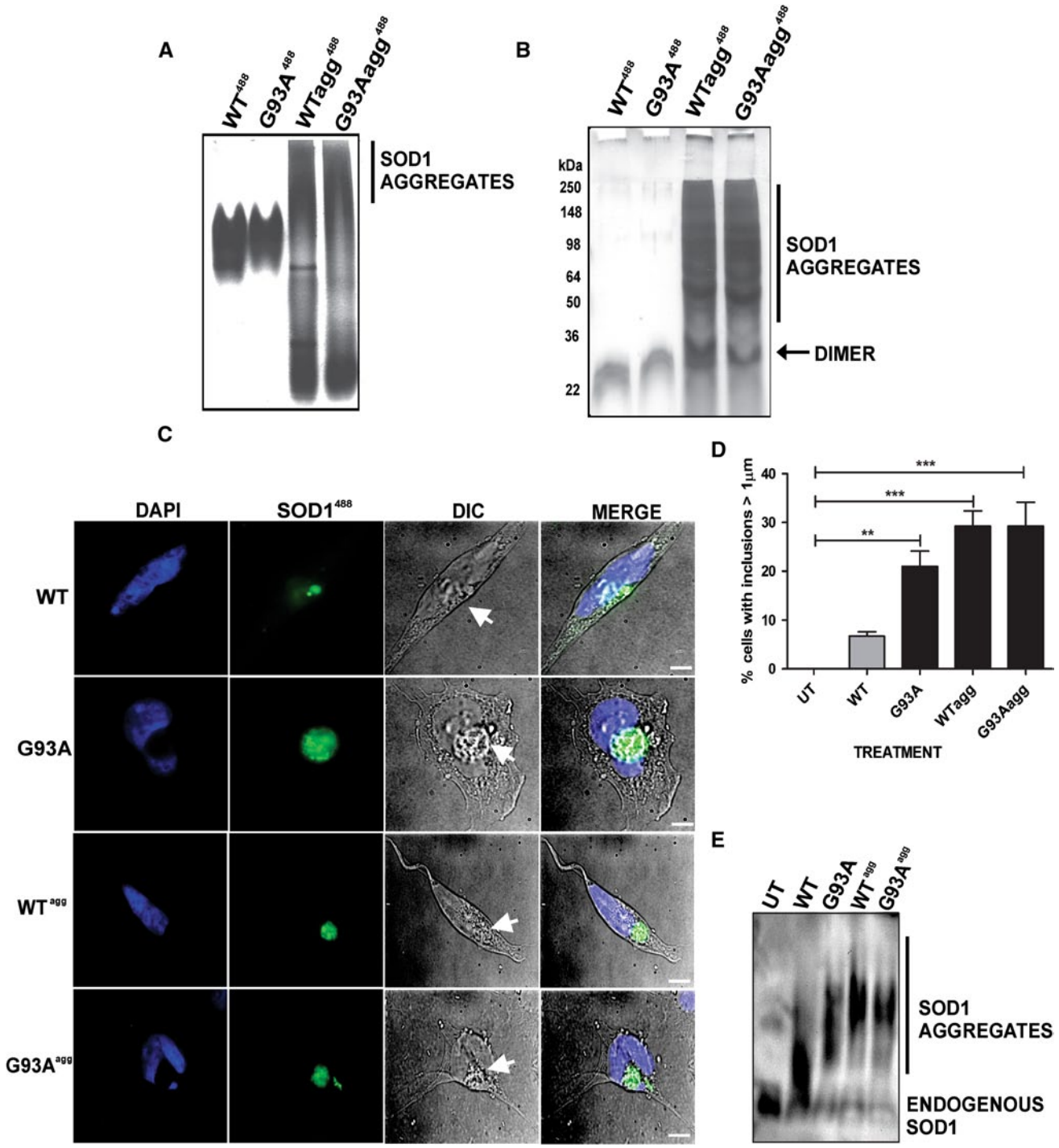

VSVG-ts045 was efficiently transported to the Golgi apparatus in untreated cells after 60 min at 32 °C. However, in cells treated with extracellular SOD1^{G93A}, aggSOD1^{WT} or aggSOD1^{G93A}, VSVG-ts045 was retained in the ER and significantly less was transported to the Golgi ($P < 0.001$) compared to untreated cells (Fig. 4a–c). Hence extracellular mutant SOD1 inhibits ER–Golgi transport similar to intracellular mutant SOD1. These findings were confirmed using NSC-34 cells treated with extracellular SOD1^{G93A} (Fig. 4d). Furthermore, aggSOD1^{WT} also inhibited ER to Golgi protein trafficking in SH-SY5Y cells, to a level comparable to both SOD1^{G93A} and aggSOD1^{G93A}. Hence both mutant and aggregated SOD1 inhibit ER–Golgi transport. There was no significant difference in the transport of VSVG-ts045 from ER–Golgi in NSC-34 cells treated with native SOD1^{WT} compared to UT cells. A slight difference was observed in SH-SY5Y cells treated with native SOD1^{WT}, but this was not statistically significant

◀ **Fig. 2** Uptake and aggregation of extracellular mutant $SOD1^{G93A}$ and aggregated $SOD1^{WT}$ in SH-SY5Y cells. **a** Recombinant purified $SOD1^{WT}$ and $SOD1^{G93A}$ proteins were aggregated by treatment with 50 mM DTT and 5 mM EDTA at 37 °C for 72 h and labeled with Alexa Fluor 488 dye. The formation of aggregates was confirmed by 10 % native gel electrophoresis (1 μg/lane) followed by silver staining. **b** Silver stained SDS PAGE of SOD1 aggregates with 100 mM Iodoacetamide, revealed the presence of SDS stable higher molecular weight $WTagg^{488}$ and $G93Aagg^{488}$ aggregates, as indicated. **c** Native and aggregated $SOD1^{WT}$ and $SOD1^{G93A}$ labeled proteins were added to the SH-SY5Y cell culture medium at a concentration of 2 μg/mL. After 48 h treatment, the cells were fixed and examined by fluorescence microscopy ($SOD1^{488}$, *green*), after staining the nuclei with DAPI (*blue*). Representative images show the uptake of extracellular protein in each case. Intracellular fluorescent SOD1 inclusions were abundant in mutant SOD1 and aggregated SOD1 treated cells, and were present in a small proportion of native $SOD1^{WT}$ treated cells. DIC images (*panel 3 from left*, *white arrows*) show the formation of membrane ruffles characteristic of macropinocytosis in each case. All *scale bars* represent 10 μm. **d** Quantification of SOD1 inclusion formation in SH-SY5Y cells 48 h after treatment (UT, $SOD1^{WT}$, $SOD1^{G93A}$, $SOD1^{WTagg}$, $SOD1^{G93Aagg}$). SOD1 inclusions were defined as fluorescent, inclusion-like structures greater than 1 μm in diameter and were quantified using ImageJ. Results are expressed as mean ± SEM; $n = 3$; $^{**}P < 0.01$, $^{***}P < 0.001$ versus UT by one-way ANOVA with Tukey's post-test. **e** Following extracellular protein treatment for 48 h, SH-SY5Y cell lysates were collected after 0.125 % trypsin digestion of cells to remove the residual extracellular SOD1 inoculum and run on 10 % native PAGE. High molecular weight intracellular SOD1 aggregates were present in all lysates except UT cells as indicated. Endogeneous human SH-SY5Y SOD1 can be seen in UT, but this band is reduced in cells treated with native $SOD1^{WT}$, indicating the recruitment of endogenous SOD1 into the high molecular weight aggregates. Similarly, this band is further decreased in cells treated with G93A, WT^{agg} and $G93A^{agg}$ compared to both UT and $SOD1^{WT}$

(Fig. 4a–c). Consistent with these findings, extracellular mutant SOD1 did not co-localise with ER markers after uptake into NSC-34 cells (Fig S4). Hence these data suggest that extracellular SOD1 triggers ER stress from the cytoplasm following uptake into neuronal cells, by inhibiting the transport of secretory proteins from the ER to Golgi.

Inhibition of ER–Golgi transport implies disruption to the secretory pathway. Hence fragmentation of the Golgi apparatus was next examined in SH-SY5Y cells treated with extracellular SOD1, by immunostaining with anti-GM130 antibody. In untreated cells the Golgi apparatus mostly localized to a compact, perinuclear ribbon. In contrast, the Golgi apparatus fragmented into condensed punctate structures in 25–40 % of cells treated with $SOD1^{G93A}$, $aggSOD1^{WT}$ and $aggSOD1^{G93A}$ (Fig. 5a, c). Similarly, Golgi fragmentation was also detected in 25 % of NSC-34 cells treated with extracellular $SOD1^{G93A}$ (Fig. 5b, d; $P < 0.05$). The Golgi was fragmented in a smaller but significant percentage of SH-SY5Y cells ($P < 0.05$) treated with native $SOD1^{WT}$, but not in NSC-34 cells treated with native $SOD1^{WT}$ (Fig. 5c, d).

Uptake of extracellular aggregated $SOD1^{WT}$ or mutant SOD1 induces cell death in SH-SY5Y cells

Prolonged ER stress and induction of CHOP implies that apoptotic cell death is triggered in cells treated with extracellular SOD1. Hence we next examined induction of apoptosis using Annexin V/propidium iodide (PI) staining by flow cytometry [37]. After 72 h treatment with extracellular SOD1, apoptotic cell death was quantified using FACS. In SH-SY5Y cells there was a significant increase ($P < 0.05$) in the percentage of cells undergoing apoptosis after treatment with $aggSOD1^{WT}$, $SOD1^{G93A}$ and $aggSOD1^{G93A}$ compared to untreated cells (Fig. 6a, b). Treatment with aggregated forms of $SOD1^{WT}$ and $SOD1^{G93A}$ induced apoptosis in a higher percentage of cells compared to the respective native forms ($P < 0.05$). Hence apoptosis is triggered by extracellular misfolded SOD1 proteins in SH-SY5Y cells. However, there were no significant differences in the percentage of cells undergoing apoptosis in NSC-34 cells after treatment with extracellular $SOD1^{WT}$ and $SOD1^{G93A}$ compared to the controls (Fig. 6c).

Discussion

This study provides clear evidence that the uptake of extracellular misfolded SOD1 into neuronal cells initiates neurodegenerative pathways reminiscent of ALS pathology. Misfolded $SOD1^{WT}$ and mutant SOD1 were taken up by neuronal cells, inducing the formation of intracellular SOD1-positive inclusions. This triggered inhibition of transport from the ER to Golgi apparatus, ER stress, fragmentation of the Golgi and neuronal cell death, implying that extracellular SOD1 may be responsible for the spread of neurodegeneration among motor neurons in ALS. Moreover, both mutant SOD1 and aggregated $SOD1^{WT}$ displayed a similar ability to induce these effects, thus providing clues into the pathology of both familial and sporadic ALS.

This study also demonstrates that the uptake of extracellular SOD1 does not depend on the presence of a mutation or aggregation. Extracellular $SOD1^{WT}$ was taken up by murine NSC-34 cells, which did not induce pathology. A previous study demonstrated that extracellular, aggregated mutant SOD1 is taken up by macropinocytosis, a mechanism of non-selective endocytosis of macromolecules from the extracellular space [1]. The findings of our study are consistent with this mechanism because both natively folded and aggregates of $SOD1^{WT}$ and mutant SOD1 were taken up to a similar degree. Also, inhibitors of macropinocytosis were able to block the uptake of $SOD1^{WT}$ and $SOD1^{G93A}$ into NSC-34 cells. Furthermore, membrane ruffles characteristic of macropinocytosis were present in SH-SY5Y cells after

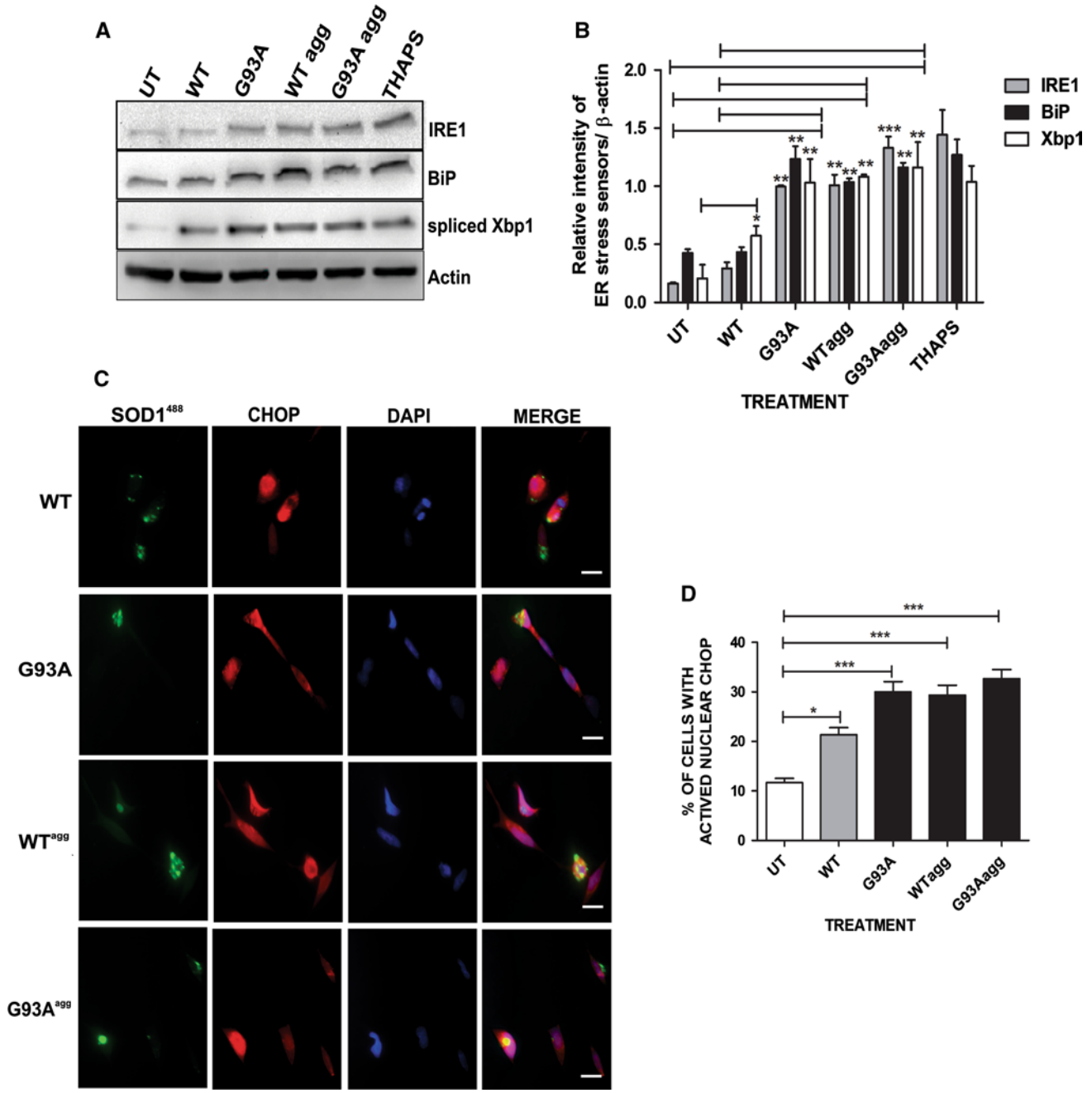

Fig. 3 Uptake of extracellular, aggregated $SOD1^{WT}$ and mutant SOD1 activates ER stress in SH-SY5Y cells. **a** Immunoblotting of cell lysates from SH-SY5Y cells treated with extracellular proteins $SOD1^{G93A}$, WT^{agg}, and $G93A^{agg}$ reveals upregulation of UPR markers IRE1, BiP, and spliced Xbp1 after 72 h treatment (20 μg/lane). As a positive control, cells were treated with 10 μM thapsigargin (THAPS) for 1 h before lysis to induce ER stress. β-actin was used as a loading control. **b** Densitometric quantification of immunoblots relative to β-actin intensity reveals upregulation of all three UPR markers in cells treated with $SOD1^{G93A}$, WT^{agg}, and $G93A^{agg}$ compared to UT cells. Results are expressed as mean ± SEM; $n = 3$; $^{*}P < 0.05$, $^{**}P < 0.01$, $^{***}P < 0.001$ versus untreated cells or $SOD1^{WT}$ treated cells as indicated, by one-way ANOVA with Tukey's post-test. **c** Representative fluorescent microscopy images demonstrate nuclear immunoreactivity to CHOP (*red*), indicating activation of CHOP and hence ER stress, 72 h after treatment with WT, G93A, WT^{agg}, $G93A^{agg}$ SOD1. All *scale bars* represent 10 μm. **d** Quantification of the proportion of SH-SY5Y cells with nuclear CHOP immunoreactivity in (**c**), 72 h after treatment with WT, G93A, WT^{agg} and $G93A^{agg}$. Results are expressed as mean ± SEM; $n = 3$; $^{*}P < 0.05$, $^{***}P < 0.001$ versus UT by one-way ANOVA with Tukey's post-test

treatment with extracellular SOD1 [38–40]. Our findings imply that secretion or simple diffusion of misfolded SOD1 into CSF by affected cells (including astrocytes and microglia, as well as motor neurons) could be subsequently endocytosed by neighboring motor neurons, thus inducing neurodegeneration. As ALS is now considered as a multi-system disorder where there is an interplay between motor neurons and other neuronal cell types [41, 42], uptake of misfolded or mutant SOD1 by neuronal cells would therefore explain the neurospatial spread of pathology in human ALS. Consistent with this notion, misfolded SOD1 has been identified in the CSF of sporadic and familial ALS patients [14, 15]. Even low levels of misfolded SOD1 in CSF could seed intracellular aggregation after uptake [14], subsequently spreading pathology.

Aggregated forms of $SOD1^{WT}$ induced similar cellular pathogenic effects to mutant SOD1 in this study. Furthermore, we observed the formation of inclusions in a small proportion of SH-SY5Y cells treated with native $SOD1^{WT}$, which were never present in NSC-34 cells. Metal-free forms of SOD1 have been proposed to be the toxic precursor preceding aggregation in familial ALS [43, 44]. The majority of ALS mutations affect the structural stability of SOD1, leading to the exposure of buried hydrophobic residues, thus resulting in aggregation [45]. Hence $SOD1^{WT}$ has an intrinsic propensity to aggregate which is enhanced by mutation. Previous studies have demonstrated that misfolded, oxidized $SOD1^{WT}$ is as pathogenic as mutant SOD1 [16]. However, we observed pathological effects induced by extracellular native $SOD1^{WT}$ in human SH-SY5Y cells not previously observed in murine NSC-34 cells or by intracellular expression of $SOD1^{WT}$. The reason for this is unclear, but it is possible that native $SOD1^{WT}$ recruits endogeneous human SOD1 into aggregates after uptake in SH-SY5Y cells. This would explain the lower but significant inclusion formation, activation of ER stress and Golgi fragmentation in SH-SY5Y cells treated with unaggregated, extracellular $SOD1^{WT}$. Both recombinant, purified $SOD1^{WT}$ from *Escherichia coli*, or Sf9 medium containing $SOD1^{WT}$, were taken up by NSC-34 cells, but neither induced ER stress, or aggregate/inclusion formation. Similarly, we detected apoptosis in SH-SY5Y cells but not NSC-34 cells treated with extracellular SOD1. These data are consistent with the notion that there is species specificity in the recruitment of SOD1 misfolding [17], thus implicating a gain of toxic function by $SOD1^{WT}$ in the presence of human SOD1. Indeed, overexpression of $SOD1^{WT}$ induces misfolding of endogenous SOD1 in the same cell line [17]. We also observed that the addition of extracellular SOD1 results in the rapid formation of intracellular SOD1 aggregates in the cytoplasm after uptake. This replicates the commonly described observation that over-expression of mutant SOD1 in cell culture results in the rapid formation of aggregates. In contrast, aggregates appear much later in mouse ALS models based on transgenic over-expression of mutant SOD1, generally at the end stages of disease [11, 46], thus highlighting differences observed between animal and cellular disease models.

ER stress is now established as a key pathway to cell death in ALS [7, 8, 23, 31]. Mutant SOD1 induces ER stress [6] and Golgi fragmentation [26] in neuronal cell cultures, and we now show that aggregated $SOD1^{WT}$ induces UPR and Golgi fragmentation similar to mutant SOD1. These findings are consistent with recent evidence for common pathogenic pathways shared by mutant SOD1 and $SOD1^{WT}$, and the presence of misfolded $SOD1^{WT}$ in sporadic ALS tissues [4, 5]. It is unclear how ER stress is triggered in ALS because SOD1 is normally located in the cytoplasm and reports that it is found in microsomes [47] have been subsequently challenged [23]. However, it was previously proposed that ER stress in ALS is triggered by cytoplasmic SOD1 [23]. We show here that extracellular SOD1 does not co-localise with ER markers after uptake, consistent with the notion that ER stress is triggered from the cytoplasm. However, ER stress can be caused by failure of ER–Golgi trafficking [24, 25]. We also confirm here that intracellular mutant SOD1 inhibits the transport of VSVG-ts045 from the ER to Golgi in SH-SY5Y cells, and we show that extracellular forms of mutant and aggregated $SOD1^{WT}$ also delay ER–Golgi traffic, thus providing one possible explanation for induction of ER stress. Similarly, Golgi fragmentation is also triggered by an imbalance between anterograde and retrograde traffic between ER and Golgi [26], highlighting a possible role for disruption to ER–Golgi traffic in both events. The activation of pro-apoptotic CHOP and increase in the proportion of cells undergoing apoptosis in cells treated with extracellular SOD1 provides a link between extracellular proteins and neurodegeneration and UPR-specific cell death. Hence this study also provides further evidence linking the disruption of ER–Golgi compartments to ALS and shows that extracellular misfolded proteins can induce dysfunction in these organelles.

In conclusion, this study establishes mechanisms of toxicity induced by extracellular SOD1 applicable to both sporadic and familial ALS. Our findings are consistent with a prion-like propagation of neurotoxicity in ALS, and they provide further evidence for common neurodegenerative pathways shared by mutant and $SOD1^{WT}$ linked to the ER–Golgi compartments. The demonstration of specific, cellular pathways targeted by extracellular, misfolded SOD1 also provides novel targets for ameliorating the spread of neurodegeneration in ALS.

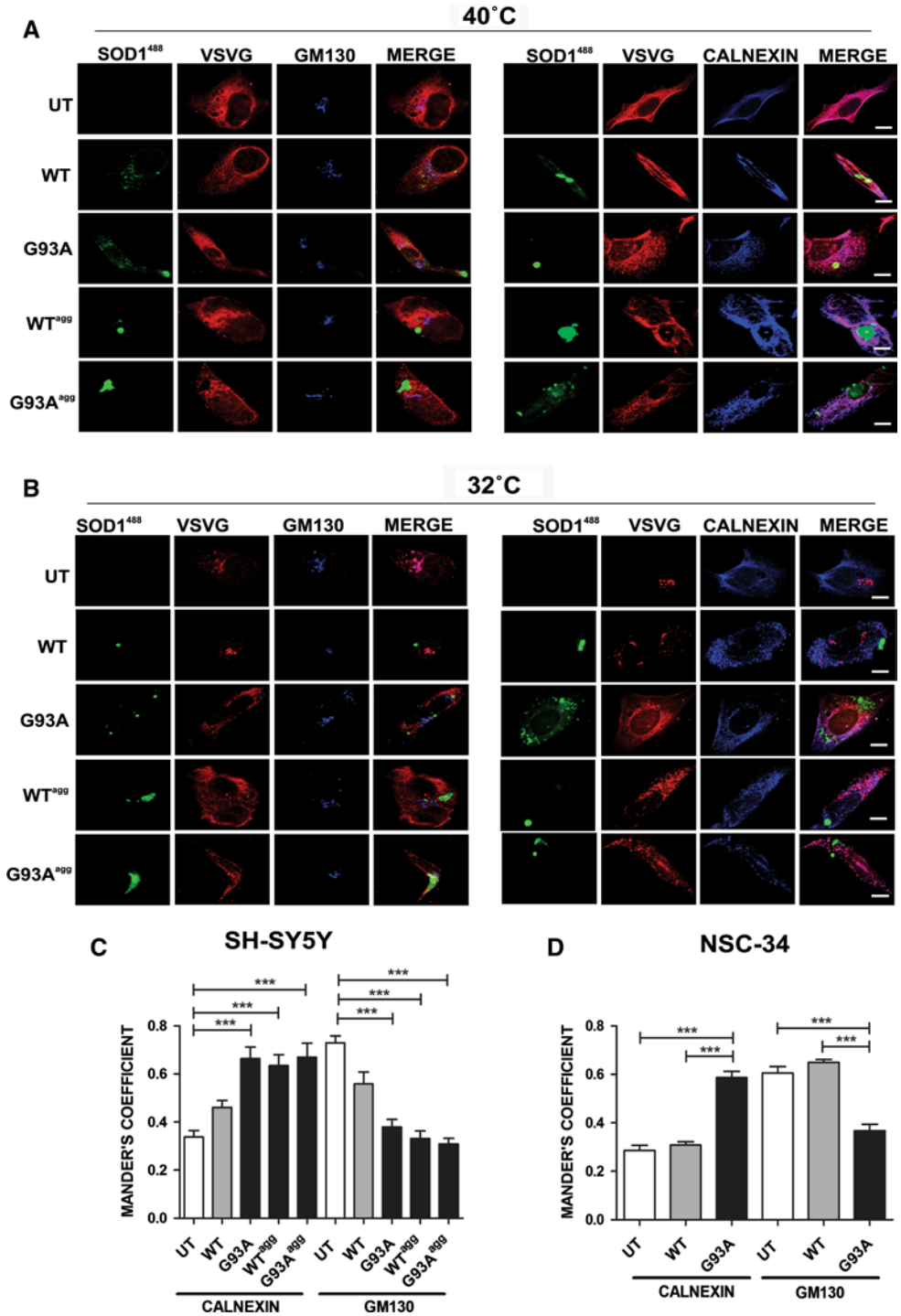

Materials and methods

Expression and purification of recombinant SOD1

Human SOD1^{WT} and SOD1^{G93A} were expressed and purified from *E. coli* as previously described [28, 48]. Briefly, *E. coli* cells were cultured at 23 °C with 3 mM $CuSO_4$ and 30 μM $ZnSO_4$ for metal loading. SOD1^{WT} and SOD1^{G93A} proteins were then purified from bacterial lysates, by heat denaturation, size exclusion chromatography (Superdex 75; GE Healthcare), and anion-exchange chromatography using a Q-Sepharose anion exchange column (GE Healthcare), and eluted with a salt gradient of 0–125 mM NaCl, pH 7.5 [28].

◀ **Fig. 4** Uptake of extracellular, aggregated WT and mutant SOD1 inhibits ER to Golgi protein trafficking in SH-SY5Y cells. Cells expressing VSVG-ts045 mCherry were treated with WT, G93A, WT^{agg}, $G93A^{agg}$ at 24 h post transfection. After trapping VSVG-ts045 mCherry in the ER by incubation at 40 °C for 24 h, the temperature was shifted to 32 °C for 60 min or fixed immediately at 0 min. The cells were then stained with calnexin (*blue*), a marker of the ER, or GM130 (*blue*), a marker of the Golgi apparatus. **a** Representative fluorescent images of cells expressing VSVG-ts045 (*red*) treated with WT, G93A, WT^{agg}, $G93A^{agg}$ SOD1 protein (*green*) and UT cells after incubation at 40 °C (0 min). **b** Representative fluorescent images after 60 min incubation at 32 °C. VSVG is co-localised with GM130 in cells treated with native $SOD1^{WT}$ and UT cells in contrast to cells treated with WT^{agg}, G93A, $G93A^{agg}$, in which VSVG is still predominantly co-localised with calnexin, indicating an inhibition of VSVG-ts045 transport from ER to Golgi. All scale bars 10 μm. **c** Quantification of the degree of co-localisation of VSVG-ts045 with calnexin and GM130 at 60 min as in **b** using Mander's coefficient. Data are presented as mean ± SEM, $***P < 0.001$ versus UT by one-way ANOVA with Tukey's post-test, $n = 3$. **d** Uptake of extracellular mutant SOD1 inhibits ER to Golgi protein trafficking in NSC-34 cells. Cells expressing VSVG-ts045 mCherry were treated with recombinant, labelled $SOD1^{WT}$ or $SOD1^{G93A}$ at 24 h post transfection. After trapping VSVG-ts045 mCherry in the ER by incubation at 40 °C for 24 h, the temperature was shifted to 32 °C for 0 and 30 min. The degree of co-localisation of VSVG-ts045 with calnexin and GM130 was quantified using Mander's coefficient. Data are presented as mean ± SEM, $***P < 0.001$ versus $SOD1^{WT}$ treated or UT cells as indicated by one-way ANOVA with Tukey's post-test, $n = 3$

Expression of SOD1 from Sf9 baculoviral system

Human $SOD1^{WT}$ and $SOD1^{G93A}$ constructs were generated by PCR and cloned into pIEX-3 plasmids using *Spe*I restriction sites. *Spodoptera frugiperda* (Sf9) cells were kindly provided by Dr. Mark Hulett, La Trobe University. The cells were cultured at 28 °C and transfected using GeneJuice transfection reagent (Invitrogen) as per the manufacturer's protocol. 48 h after transfection the culture medium was collected after centrifugation at 1200 rpm for 5 min and analyzed by immunoblotting.

Zymography–SOD1 activity assay

For zymography, SOD1 protein samples were electrophoresed on a 10 % native PAGE. The gel was then soaked in 2.45 mM nitro blue tetrazolium (Sigma) for 20 min, washed with dH_2O and soaked in developer solution containing 28 mM tetramethylehylenediamine (TEMED; BIO-RAD), 28 μM riboflavin, and 36 mM KH_2PO_4 (Sigma) for 15 min. The gel was illuminated for 5–15 min until sufficient contrast between achromatic zones and blue background was achieved.

Aggregation and labeling of $SOD1^{WT}$ and mutant $SOD1^{G93A}$

In vitro SOD1 aggregation was performed as previously described [28]. Purified $SOD1^{WT}$ and G93A SOD1 proteins (1 mg/mL) dissolved in PBS were incubated with 50 mM dithiothreitol (DTT) and 5 mM ethylenediaminetetraacetic acid (EDTA) at 37 °C for 72 h whilst shaking and vortexed briefly to obtain a homogenous solution. Aggregated and native $SOD1^{WT}$ and $SOD1^{G93A}$ were then labeled using the Alexa Fluor 488 Microscale Protein Labeling Kit (Invitrogen). Protein (100 μg) was incubated with dye in the presence of 100 mM $NaHCO_3$ at room temp for 15 min. The unlabeled protein was then separated using Amicon Ultra 10 kDa centrifugal filters (Millipore).

Extracellular SOD1 treatment

Mouse motor neuron-like NSC-34 or human neuroblastoma SH-SY5Y cells were cultured on 24 well plates with or without 13 mm coverslips at 10^5 cells/well. Purified recombinant SOD1 (2 μg/mL) expressed in bacteria was added to the culture medium 24 h after seeding, and 48 h later the cells were analyzed by immunocytochemistry or immunoblotting. For cells treated with Sf9 conditioned medium containing GST-SOD1 or GST-only control, medium containing 100 μg total protein was added to the NSC-34 culture medium to a final concentration of 0.2 mg/mL.

SOD1 uptake and inhibition

NSC34 cells were cultured on coverslips for 24 h before treatment with either 3 μM rottlerin D, 100 μM EIPA, 10 μM genistein or 5 μM chlorpromazine HCL for 30 min at 4 °C. These cells were then treated with $SOD1^{WT}$ or $SOD1^{G93A}$ or untreated at 4 °C for 30 min before being washed with PBS. The cells were then fixed with 4 % PFA and incubated with 0.5 % BSA in PBS for 20 min at room temperature. A 1:500 dilution of anti-human SOD1 sheep antiserum (Thermo Fisher Scientific) in PBS containing 0.1 % BSA and subsequent goat anti-sheep Alexa488 (Invitrogen) was used to detect internalized SOD1. SOD1 was visualized using a Leica SP5 scanning confocal microscope.

Immunocytochemistry

NSC-34 or SH-SY5Y cells grown on coverslips were washed with PBS and fixed with 4 % paraformaldehyde (PFA; Merck) in PBS for 10 min. Cells were permeabilized in 0.1 % Triton X-100 in PBS for 2 min, blocked for 30 min with 1 % BSA in PBS and incubated with the appropriate primary antibodies as follows for 16 h at 4 °C: anti-CHOP (1:50; Santa Cruz), anti-GM130 (1:50; BD Transduction Laboratories™), anti-Calnexin (1:100; Abcam) or anti-GST (MBB lab; La Trobe University). Secondary AlexaFluor-594 or 644 conjugated anti-mouse or anti-Rabbit antibodies (1:2000; Molecular Probes) were incubated for

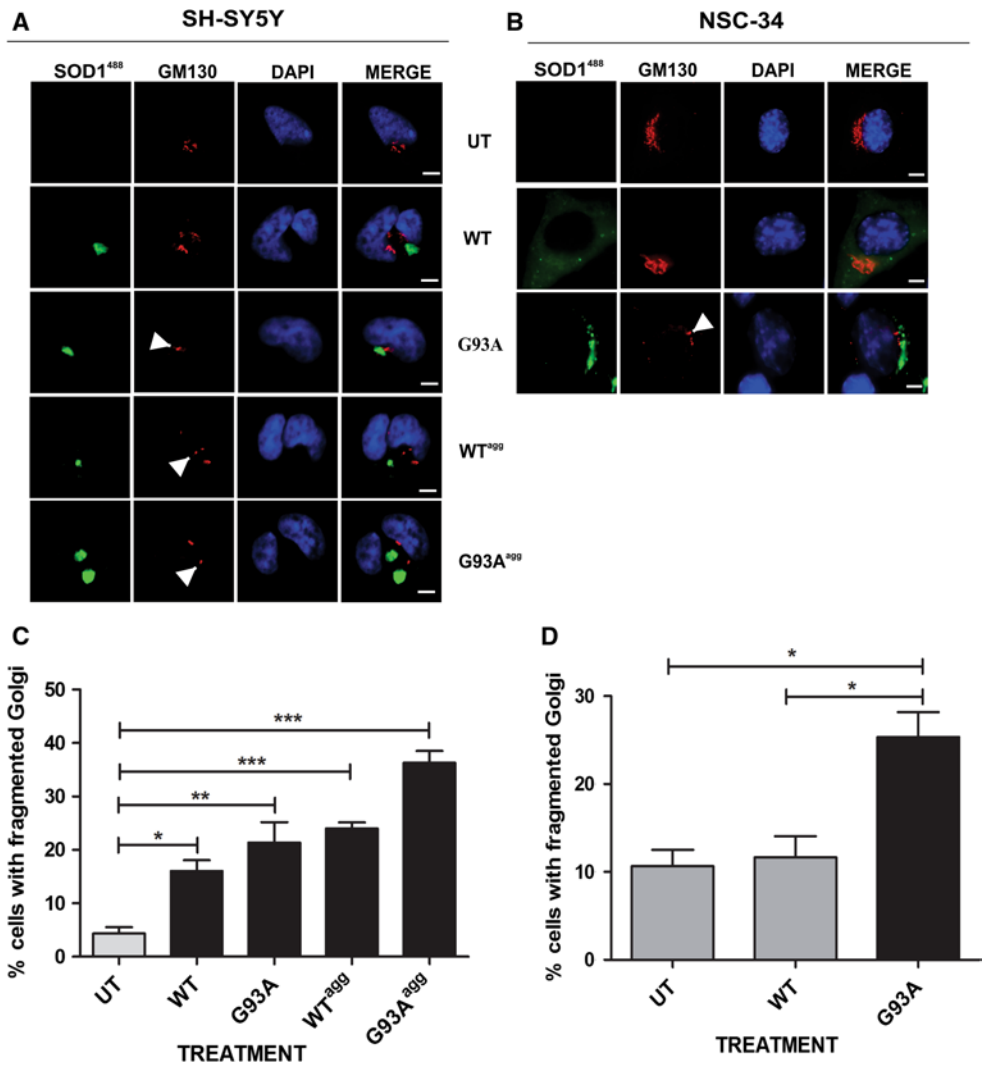

Fig. 5 Uptake of extracellular, aggregated $SOD1^{WT}$ and mutant SOD1 induces Golgi fragmentation in SH-SY5Y and NSC-34 cells. SH-SY5Y cells treated with extracellular WT, G93A, WT^{agg}, $G93A^{agg}$ SOD1 or NSC-34 cells treated with $SOD1^{WT}$ and $SOD1^{G93A}$ were fixed with 4 % PFA after 72 h treatment and immunostained with anti-GM130 antibody. **a** Representative images of SH-SY5Y cells treated with WT, G93A, WT^{agg}, $G93A^{agg}$ SOD1 (*green*). Cells were stained with anti-GM130 antibody (*red*) and nuclei were stained with DAPI (*blue*). *Arrows* indicate fragmented Golgi, indicated by condensed punctate structures in contrast to intact Golgi (UT cells). **b** Representative images of NSC-34 cells stained with GM130 (*red*) showing fragmented Golgi after treatment with mutant $SOD1^{G93A}$. All *scale bars* represent 10 μm. **c** Quantification of cells with fragmented Golgi in SH-SY5Y cells upon treatment with extracellular WT, G93A, WT^{agg}, $G93A^{agg}$ SOD1 for 72 h. **d** Quantification of cells with fragmented Golgi in NSC-34 cells 72 h after treatment with extracellular $SOD1^{WT}$ and $SOD1^{G93A}$. There is no significant difference in the proportion of NSC-34 cells with fragmented Golgi in extracellular $SOD1^{WT}$ treated cells compared to UT cells, in contrast to SH-SY5Y cells. Results are expressed as mean ± SEM; $n = 3$; $^{*}P < 0.05$, $^{**}P < 0.01$, $^{***}P < 0.001$ versus UT cells by one-way ANOVA with Tukey's post-test

1 h at room temperature, cells were then treated with Hoechst 33342 (Invitrogen) and mounted on slides using fluorescent mounting medium (Dako). Images were acquired using constant gain and offset settings for CHOP using an Olympus fluorescence microscope at 40× magnification. Induction of ER stress was assessed by examining individual cells for nuclear immunoreactivity to CHOP. For each treatment, 100 cells from three different experiments were scored. Fragmentation of the Golgi apparatus was determined by staining with the anti-GM130 antibody. The number of cells with fragmented Golgi per 100 cells from three different experiments was scored by fluorescence microscopy.

Protein extraction

The cells were washed with PBS and lysed with TN buffer (50 mM Tris–HCl pH 7.5, 150 mM NaCl, 0.1 % SDS) with

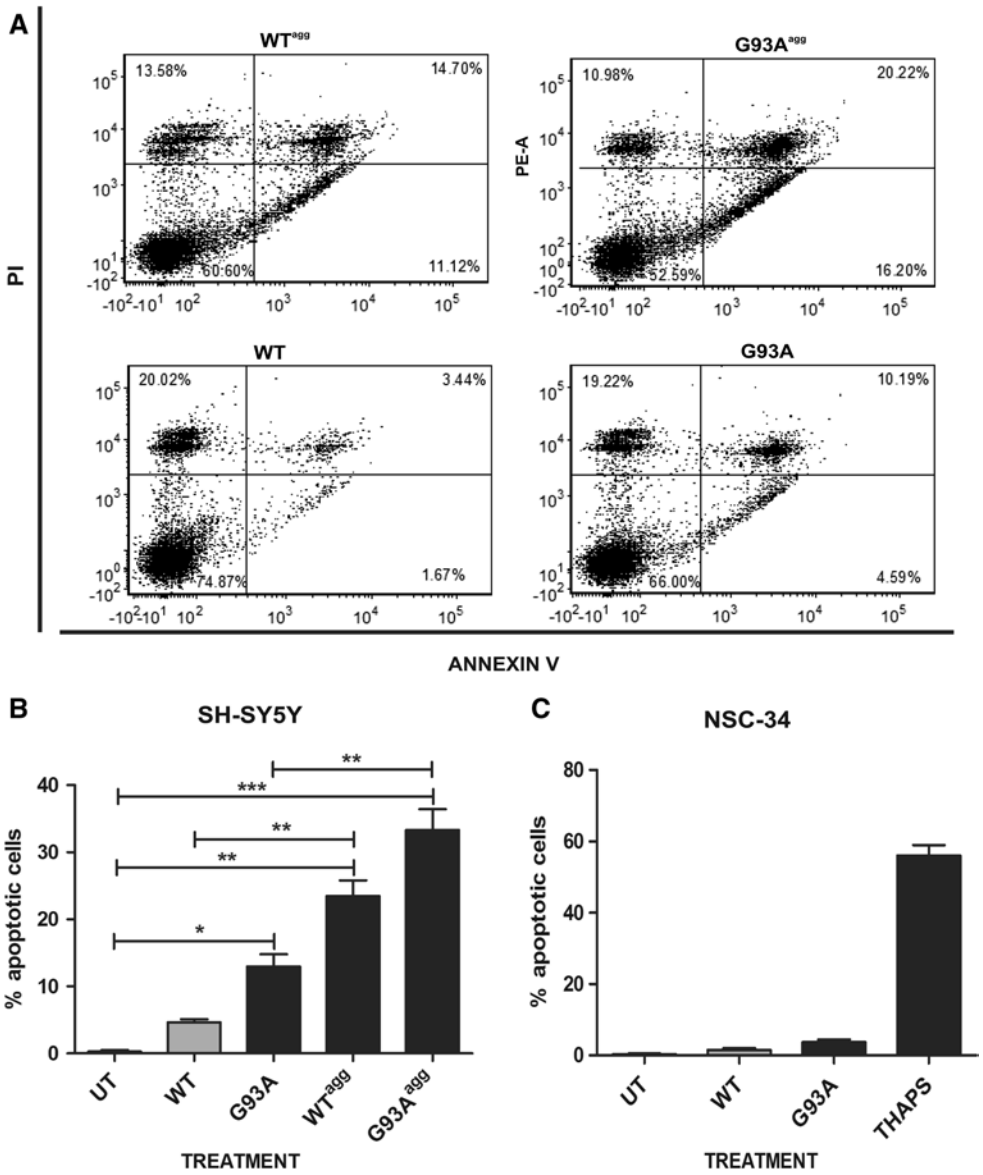

Fig. 6 Uptake of extracellular aggregated $SOD1^{WT}$ and mutant SOD1 induces apoptotic cell death in SH-SY5Y cells but not NSC-34 cells. **a** SH-SY5Y cells treated with extracellular WT, G93A, WT^{agg} and $G93A^{agg}$ SOD1 for 72 h were harvested, stained with PI/Annexin V and the percentage of cells in both early and late apoptotic phase was gated and scored by flow cytometry, as indicated by cells stained with both PI and Annexin V. **b** Percentage of apoptotic cells among cells treated with WT, G93A, WT^{agg} and $G93A^{agg}$ and UT cells. Results are expressed as mean ± SEM; $n = 3$; $^{*}P < 0.05$, $^{**}P < 0.01$, $^{***}P < 0.001$ versus untreated cells by one-way ANOVA with Tukey's post-test, $n = 3$. **c** NSC-34 cells treated with extracellular $SOD1^{WT}$ and $SOD1^{G93A}$ for 72 h were stained with PI/Annexin V and analysed by flow cytometry. Incontrast to SH-SY5Y cells, no significant percentage (>5 %) of apoptotic cells were identified in NSC-34 after treatment with $SOD1^{G93A}$. NSC-34 cells were treated with 10 μM thapsigargin (THAPS) for 4 h before harvesting as a positive control

1 % protease inhibitor (Sigma), followed by incubation on ice for 10 min. The SDS soluble protein fraction was collected by centrifugation at 16 100 *g* for 10 min. For immunoblotting, the cells were also treated with 0.125 % trypsin for 2 min at room temperature before lysis, to remove residual extracellular SOD1.

Immunoblotting

Protein samples (20 μg) electrophoresed through 10 % SDS–polyacrylamide gels or 10 % native PAGE (non-denaturing) gels and transferred to nitrocellulose membranes (Millipore). For the SDS-PAGE analysis of SOD1 aggregates, the samples were prepared in sample loading buffer (0.042 M Tris–HCl, 2 % SDS, 1 % glycine, 0.005 % bromophenol blue, 10 % glycerol, 100 mM iodoacetamide, 4 % freshly added β mercaptoethanol). Membranes were blocked with 3 % (w/v) bovine serum albumin (BSA; Sigma), pH 8.0 for 1 h. The appropriate primary antibodies were prepared in 1 % (w/v) BSA solution as follows: SOD1 (1:1000; Calbiochem), BiP (1:4000; Stressgen), Xbp1 (1:400; SC), IRE1 (1:600; SC) and β actin as a loading control (1:750; Sigma-Aldrich). All antibodies were incubated with membranes for 1 h at room temperature (RT). Blots were probed with HRP-conjugated donkey anti-sheep, goat anti-rabbit or goat anti-mouse antibodies at 1:2500 (Chemicon) for 1 h at RT and then developed using enhanced chemiluminescence (ECL) reagents (Roche). Quantification of band intensities was performed by densitometric analysis following subtraction of background using Image J (National Institutes of Health, Bethesda, MA, USA) and expressed relative to the corresponding signal for β-actin.

Blots were stripped using Reblot Plus solution (Chemicon) for 15 min, and then reprobed as above.

VSVG transport assay

SH-SY5Y or NSC-34 cells were plated on 24-well plates with 13 mm coverslips. After 24 h in culture, cells were transfected with VSVG-ts045 tagged with fluorescent mCherry (a kind gift from Dr. Jennifer Lippincott-Schwartz and Dr. George Patterson) and another 24 h later cells were treated with extracellular SOD1 protein [35]. Following treatment for 24 h, cells were incubated at 40 °C for 24 h to accumulate VSVG-ts045 in the ER. Cycloheximide (20 μg/mL) was then added, and cells were shifted to 32 °C for 60 min or immediately fixed at 0 min. At each time interval, cells were washed with ice-cold PBS and fixed with 4 % PFA. The ER and Golgi compartments were immunostained with rabbit polyclonal anti-Calnexin antibody (Abcam) and mouse monoclonal anti-GM130 antibody (BD Transduction Laboratories™) as described above. In each experiment 20 cells were scored, and all experiments were performed in triplicate. Image analysis was performed using Image J using the JACoP plugin to threshold and collect the Mander's coefficient [36] between the mCherry and far-red channels.

Annexin V binding assay to detect apoptotic cell death

SH-SY5Y cells cultured in six-well plates were treated with extracellular SOD1 protein as above. The cells were harvested after 72 h treatment by adding trypsin for 1 min at room temperature. The cells were then collected in PBS, centrifuged at 1200 rpm for 5 min, and resuspended in 200 μl of annexin V binding buffer (10 mM HEPES, 140 mM NaCl, 2.5 mM $CaCl_2$, pH 7.4). The cell suspension was treated with 3 μl of annexin V dye (Invitrogen) at room temperature for 15 min in the dark. Annexin V binding buffer (100 μl) was then added to the cell suspension, counter-stained with 5 μg/mL of propidium iodide (PI, Sigma) and analyzed by BD FACS Canto II flow cytometer.

Statistical analyses

Data are presented as mean ± standard error of the mean (SEM) from at least three independent experiments and were analyzed by one-way ANOVA followed by Tukey's post hoc test using Prism 5.0 GraphPad Software. A value of $P < 0.05$ was considered significant.

Acknowledgments We thank Professor Neil Cashmann for the gift of NSC-34 cells, and we thank Dr Jennifer Lippincott-Schwartz and Dr George Patterson for the VSVG-ts045-mCherry construct. This work was supported by National Health and Medical Research Council of Australia Project Grants [# 1006141, 1030513 to J.A.], Bethlehem Griffiths Research Foundation, Motor Neuron Disease Research Institute of Australia, Suzie Harris Memorial Fund MND Research Grant and Rosalind Nicholson MND Research Grant [to J.A.], a National Health and Medical Research Council CJ Martin Biomedical Early Career fellowship [1036835 to A.W.] and an Australian Postgraduate Award and Australian Rotary Health scholarship [to A.W.].

References

1. Münch C, O'Brien J, Bertolotti A (2011) Prion-like propagation of mutant superoxide dismutase-1 misfolding in neuronal cells. Proc Natl Acad Sci USA 108:3548–3553
2. Desplats P, Lee HJ, Bae EJ, Patrick C, Rockenstein E, Crews L, Spencer B, Masliah E, Lee SJ (2009) Inclusion formation and neuronal cell death through neuron-to-neuron transmission of α-synuclein. Proc Natl Acad Sci USA 106(31):13010–13015
3. Clavaguera F, Bolmont T, Crowther RA, Abramowski D, Frank S, Probst A, Fraser G, Stalder AK, Beibel M, Staufenbiel M (2009) Transmission and spreading of tauopathy in transgenic mouse brain. Nat Cell Biol 11(7):909–913
4. Bosco DA, Morfini G, Karabacak NM, Song Y, Gros-Louis F, Pasinelli P, Goolsby H, Fontaine BA, Lemay N, McKenna-Yasek D (2010) Wild-type and mutant SOD1 share an aberrant conformation and a common pathogenic pathway in ALS. Nat Neurosci 13(11):1396–1403
5. Forsberg K, Jonsson PA, Andersen PM, Bergemalm D, Graffmo KS, Hultdin M, Jacobsson J, Rosquist R, Marklund SL, Brännström T (2010) Novel antibodies reveal inclusions containing non-native SOD1 in sporadic ALS patients. PLoS ONE 5(7):e11552
6. Atkin JD, Farg MA, Turner BJ, Tomas D, Lysaght JA, Nunan J, Rembach A, Nagley P, Beart PM, Cheema SS (2006) Induction of the unfolded protein response in familial amyotrophic lateral sclerosis and association of protein-disulfide isomerase with superoxide dismutase 1. J Biol Chem 281(40):30152–30165
7. Atkin JD, Farg MA, Walker AK, McLean C, Tomas D, Horne MK (2008) Endoplasmic reticulum stress and induction of the unfolded protein response in human sporadic amyotrophic lateral sclerosis. Neurobiol Dis 30(3):400–407
8. Saxena S, Cabuy E, Caroni P (2009) A role for motoneuron subtype-selective ER stress in disease manifestations of FALS mice. Nat Neurosci 12(5):627–636
9. Gonatas N, Stieber A, Mourelatos Z, Chen Y, Gonatas J, Appel S, Hays A, Hickey W, Hauw J (1992) Fragmentation of the Golgi apparatus of motor neurons in amyotrophic lateral sclerosis. Am J Pathol 140(3):731
10. Guareschi S, Cova E, Cereda C, Ceroni M, Donetti E, Bosco DA, Trotti D, Pasinelli P (2012) An over-oxidized form of superoxide dismutase found in sporadic amyotrophic lateral sclerosis with bulbar onset shares a toxic mechanism with mutant SOD1. Proc Natl Acad Sci USA 109(13):5074–5079
11. Graffmo KS, Forsberg K, Bergh J, Birve A, Zetterström P, Andersen PM, Marklund SL, Brännström T (2013) Expression of wild-type human superoxide dismutase-1 in mice causes amyotrophic lateral sclerosis. Hum Mol Genet 22(1):51–60
12. Turner BJ, Atkin JD, Farg MA, Rembach A, Lopes EC, Patch JD, Hill AF, Cheema SS (2005) Impaired extracellular secretion of mutant superoxide dismutase 1 associates with neurotoxicity in familial amyotrophic lateral sclerosis. J Neurosci 25(1):108–117
13. Gomes C, Keller S, Altevogt P, Costa J (2007) Evidence for secretion of Cu, Zn superoxide dismutase via exosomes from

a cell model of amyotrophic lateral sclerosis. Neurosci Lett 428(1):43–46
14. Frutiger K, Lukas TJ, Gorrie G, Ajroud-Driss S, Siddique T (2008) Gender difference in levels of Cu/Zn superoxide dismutase (SOD1) in cerebrospinal fluid of patients with amyotrophic lateral sclerosis. Amyotrophic Lateral Scler 9(3):184–187
15. Zetterström P, Andersen PM, Brännström T, Marklund SL (2011) Misfolded superoxide dismutase-1 in CSF from amyotrophic lateral sclerosis patients. J Neurochem 117(1):91–99
16. Ezzi SA, Urushitani M, Julien JP (2007) Wild type superoxide dismutase acquires binding and toxic properties of ALS linked mutant forms through oxidation. J Neurochem 102(1):170–178
17. Grad LI, Guest WC, Yanai A, Pokrishevsky E, O'Neill MA, Gibbs E, Semenchenko V, Yousefi M, Wishart DS, Plotkin SS (2011) Intermolecular transmission of superoxide dismutase 1 misfolding in living cells. Proc Natl Acad Sci 108(39):16398–16403
18. Urushitani M, Ezzi SA, Julien JP (2007) Therapeutic effects of immunization with mutant superoxide dismutase in mice models of amyotrophic lateral sclerosis. Proc Natl Acad Sci 104(7):2495–2500
19. Gros-Louis F, Soucy G, Larivière R, Julien JP (2010) Intracerebroventricular infusion of monoclonal antibody or its derived Fab fragment against misfolded forms of SOD1 mutant delays mortality in a mouse model of ALS. J Neurochem 113(5):1188–1199
20. Takeuchi S, Fujiwara N, Ido A, Oono M, Takeuchi Y, Tateno M, Suzuki K, Takahashi R, Tooyama I, Taniguchi N (2010) Induction of protective immunity by vaccination with wild-type apo superoxide dismutase 1 in mutant SOD1 transgenic mice. J Neuropathol Exp Neurol 69(10):1044
21. Ron D, Walter P (2007) Signal integration in the endoplasmic reticulum unfolded protein response. Nat Rev Mol Cell Biol 8(7):519–529
22. Bertolotti A, Zhang Y, Hendershot LM, Harding HP, Ron D (2000) Dynamic interaction of BiP and ER stress transducers in the unfolded-protein response. Nat Cell Biol 2(6):326–332
23. Nishitoh H, Kadowaki H, Nagai A, Maruyama T, Yokota T, Fukutomi H, Noguchi T, Matsuzawa A, Takeda K, Ichijo H (2008) ALS-linked mutant SOD1 induces ER stress-and ASK1-dependent motor neuron death by targeting Derlin-1. Genes Dev 22(11):1451–1464
24. Preston A, Gurisik E, Bartley C, Laybutt D, Biden T (2009) Reduced endoplasmic reticulum (ER)-to-Golgi protein trafficking contributes to ER stress in lipotoxic mouse beta cells by promoting protein overload. Diabetologia 52(11):2369–2373
25. Thayanidhi N, Helm JR, Nycz DC, Bentley M, Liang Y, Hay JC (2010) α-Synuclein delays endoplasmic reticulum (ER)-to-Golgi transport in mammalian cells by antagonizing ER/Golgi SNAREs. Mol Biol Cell 21(11):1850–1863
26. Mourelatos Z, Gonatas NK, Stieber A, Gurney ME, Dal Canto MC (1996) The Golgi apparatus of spinal cord motor neurons in transgenic mice expressing mutant Cu, Zn superoxide dismutase becomes fragmented in early, preclinical stages of the disease. Proc Natl Acad Sci 93(11):5472–5477
27. Lucocq J, Warren G, Pryde J (1991) Okadaic acid induces Golgi apparatus fragmentation and arrest of intracellular transport. J Cell Sci 100(4):753–759
28. Roberts K, Zeineddine R, Corcoran L, Li W, Campbell IL, Yerbury JJ (2012) Extracellular aggregated Cu/Zn superoxide dismutase activates microglia to give a cytotoxic phenotype. Glia 61:409–419
29. Olczak M, Olczak T (2006) Comparison of different signal peptides for protein secretion in nonlytic insect cell system. Anal Biochem 359(1):45–53
30. Schröder M, Kaufman RJ (2005) ER stress and the unfolded protein response. Mutat Res Fundam Mol Mech Mugag 569(1):29–63
31. Walker AK, Farg MA, Bye CR, McLean CA, Horne MK, Atkin JD (2010) Protein disulphide isomerase protects against protein aggregation and is S-nitrosylated in amyotrophic lateral sclerosis. Brain 133(1):105–116
32. Furukawa Y, Kaneko K, Yamanaka K, O'Halloran TV, Nukina N (2008) Complete loss of post-translational modifications triggers fibrillar aggregation of SOD1 in the familial form of amyotrophic lateral sclerosis. J Biol Chem 283(35):24167–24176
33. Durer ZAO, Cohlberg JA, Dinh P, Padua S, Ehrenclou K, Downes S, Tan JK, Nakano Y, Bowman CJ, Hoskins JL (2009) Loss of metal ions, disulfide reduction and mutations related to familial ALS promote formation of amyloid-like aggregates from superoxide dismutase. PLoS ONE 4(3):e5004
34. Furukawa Y, Kaneko K, Yamanaka K, Nukina N (2010) Mutation-dependent polymorphism of Cu, Zn-superoxide dismutase aggregates in the familial form of amyotrophic lateral sclerosis. J Biol Chem 285(29):22221–22231
35. Hirschberg K, Miller CM, Ellenberg J, Presley JF, Siggia ED, Phair RD, Lippincott-Schwartz J (1998) Kinetic analysis of secretory protein traffic and characterization of Golgi to plasma membrane transport intermediates in living cells. J Cell Biol 143(6):1485–1503
36. Manders E, Verbeek F, Aten J (2011) Measurement of co-localization of objects in dual-colour confocal images. J Microsc 169(3):375–382
37. Darzynkiewicz Z, Juan G, Li X, Gorczyca W, Murakami T, Traganos F (1997) Cytometry in cell necrobiology: analysis of apoptosis and accidental cell death (necrosis). Cytometry 27(1):1–20
38. Doherty GJ, McMahon HT (2009) Mechanisms of endocytosis. Annu Rev Biochem 78:857–902
39. Sun P, Yamamoto H, Suetsugu S, Miki H, Takenawa T, Endo T (2003) Small GTPase Rah/Rab34 is associated with membrane ruffles and macropinosomes and promotes macropinosome formation. J Biol Chem 278(6):4063–4071
40. Grimmer S, van Deurs B, Sandvig K (2002) Membrane ruffling and macropinocytosis in A431 cells require cholesterol. J Cell Sci 115(14):2953–2962
41. Phatnani HP, Guarnieri P, Friedman BA, Carrasco MA, Muratet M, O'Keeffe S, Nwakeze C, Pauli-Behn F, Newberry KM, Meadows SK (2013) Intricate interplay between astrocytes and motor neurons in ALS. Proc Natl Acad Sci 110(8):E756–E765
42. Nagai M, Re DB, Nagata T, Chalazonitis A, Jessell TM, Wichterle H, Przedborski S (2007) Astrocytes expressing ALS-linked mutated SOD1 release factors selectively toxic to motor neurons. Nat Neurosci 10(5):615–622
43. Brotherton TE, Li Y, Cooper D, Gearing M, Julien JP, Rothstein JD, Boylan K, Glass JD (2012) Localization of a toxic form of superoxide dismutase 1 protein to pathologically affected tissues in familial ALS. Proc Natl Acad Sci 109(14):5505–5510
44. Banci L, Bertini I, Boca M, Girotto S, Martinelli M, Valentine JS, Vieru M (2008) SOD1 and amyotrophic lateral sclerosis: mutations and oligomerization. PLoS ONE 3(2):e1677
45. Tiwari A, Hayward LJ (2003) Familial amyotrophic lateral sclerosis mutants of copper/zinc superoxide dismutase are susceptible to disulfide reduction. J Biol Chem 278(8):5984–5992
46. Gurney ME, Pu H, Chiu AY, Dal Canto MC, Polchow CY, Alexander DD, Caliendo J, Hentati A, Kwon YW, Deng H-X (1994) Motor neuron degeneration in mice that express a human Cu, Zn superoxide dismutase mutation. Science 264(5166):1772–1775
47. Kikuchi H, Almer G, Yamashita S, Guégan C, Nagai M, Xu Z, Sosunov AA, McKhann GM II, Przedborski S (2006) Spinal cord endoplasmic reticulum stress associated with a microsomal accumulation of mutant superoxide dismutase-1 in an ALS model. Proc Natl Acad Sci 103(15):6025–6030
48. Lindberg MJ, Tibell L, Oliveberg M (2002) Common denominator of Cu/Zn superoxide dismutase mutants associated with amyotrophic lateral sclerosis: decreased stability of the apo state. Proc Natl Acad Sci 99(26):16607–16612